JOURNAL OF ENVIRONMENTAL SCIENCES 98 (2020) 77–84

Available online at www.sciencedirect.com

ScienceDirect

www.elsevier.com/locate/jes

JES JOURNAL OF ENVIRONMENTAL SCIENCES

www.jesc.ac.cn

Influence of incorporating beta zeolite nanoparticles on water permeability and ion selectivity of polyamide nanofiltration membranes

Baoleerhu Borjigin[1,3], *lixue Liu*[1], *Ling Yu*[1,3], *Lili Xu*[1,2], *Changwei Zhao*[1,2,*], *Jun Wang*[1,2,3,*]

[1] *State Key Laboratory of Environmental Aquatic Chemistry, Research Center for Eco-Environmental Sciences, Chinese Academy of Sciences, Beijing 100085, China*

[2] *National Engineering Laboratory for Industrial Wastewater Treatment, Research Center for Eco-Environmental Sciences, Chinese Academy of Sciences, Beijing 100085, China*

[3] *University of Chinese Academy of Sciences, Beijing 100049, China*

ARTICLE INFO

Article history:
Received 7 February 2020
Revised 31 March 2020
Accepted 9 April 2020
Available online 14 June 2020

Keywords:
β zeolite
Nanofiltration membrane
Interfacial polymerization
High flux

ABSTRACT

A novel polyamide (PA) thin film nanocomposite (TFN) membrane modified with Beta (β) zeolite was prepared by interfacial polymerization on a poly (ether sulfone) (PES) ultrafiltration membrane. Compared with the PA thin film composite (TFC) membrane, the introduction of β zeolite with porous structure notably increased the water flux of TFN membrane. Because the β zeolite with tiny-sized and well-defined inner-porous acted as prior flow channels for water molecules and a barrier for the sulfate ions. The successful introduction of β zeolite into the (PA) selective layer and their dispersion in the corresponding layer were verified by scanning electron microscope (SEM) and atomic force microscopy (AFM). Water contact angle, zeta potential measurements were used to characterize the changes of membrane surface properties before and after incorporating the β zeolite. With the β zeolite introducing, the water contact angle of modified TFN membrane was decreased to 47.8°, which was benefited to improve the water flux. Meanwhile, the negative charges of the modified TFN membrane was increased, resulting in an enhancement of separation effect on SO_4^{2-} and Cl^-. In term of nanofiltration (NF) experiments, the highest pure water flux of the TFN membranes reached up to 81.22 L m^{-2} hr^{-1} under operating pressure of 0.2 MPa, which was 2.5 times as much as the pristine TFC membrane.

Introduction

As water resources become increasingly polluted by human activities, it is a difficult challenge to provide sufficient clean water supplies to meet increasing demand for domestic use (Zhou et al., 2015). Hence, it is urgent to find an appropriate way to obtain the clean water (Lyu et al., 2015). This situation has generated noteworthy demands for the development of membrane technologies. Membrane separation technology is widely used in desalination, food production, pharmaceutical and biological industry owing to its advantages of high-efficiency, convenient operation, simple process and no biological activity loss (Lau et al., 2015). As one of the promising membrane separation technologies, NF has received wide attention because of its versatility. NF is a pressure-driven membrane separation technology between ultrafiltration (UF) and

* Corresponding authors.
E-mails: zhaocw@rcees.ac.cn (C. Zhao), junwang@rcees.ac.cn (J. Wang).

https://doi.org/10.1016/j.jes.2020.04.010
1001-0742/

Table 1 – The TFC and TFN membranes prepared at different monomer concentrations.

Membrane	PIP in water (%)	TMC in organic phase (wt%)	β in water phase (wt%)
TFC	1%	0.2%	0
TFN0.5%	1%	0.2%	0.5%
TFN1%	1%	0.2%	1%
TFN1.5%	1%	0.2%	1.5%
TFN2%	1%	0.2%	2%
TFN2.5%	1%	0.2%	2.5%

reverse osmosis (RO). NF possesses higher rejection to more kinds of organic and inorganic substances than UF with its appropriate pore size and surface charge property (Oatley-radcli et al., 2017). Meanwhile NF typically have high rejections of multivalent inorganic salts at modest pressures. Those advantages make the NF process highly competitive according to selectivity and cost benefit compared with RO (Mohammad et al., 2015). Therefore, the development of NF has won its popularity and recognition worldwide in recent years.

NF membrane material is very important during NF water treatment process, typical NF membrane with TFC structure have been prepared by interfacial polymerization (IP) of diamine and acyl chloride. NF membrane fabricated by IP method has a dense thin PA layer on the porous substrate, which contributed to the high selectivity and water permeability (Lau et al., 2015), and optimizing the surface morphology and structure of PA layer became the common strategy to enhance the membrane performance (Ahmad et al., 2013). In recent days, many previous studies have focused on improving the separation performance by modifying the PA selective vlayer (Heinz et al., 2017; Kango et al., 2013; Lalia et al., 2013). Inorganic nanomaterials, such as silver (Andrade et al., 2015), titanium dioxide (Rajaeian et al., 2013), titanate (Sumisha et al., 2015), zirconia (Lv et al., 2016) and silicon dioxide (Wei et al., 2019), have been found to improve the separation performance of membranes, when they are introduced into IP process to form a thin-film nanocomposite. These nanomaterials optimized the membrane properties including surface hydrophilicity, charge, and salt rejection.

Among various nanoparticles, zeolite nanoparticles are one of the ideal additives because of its unique properties, such as their high specific surface area, large pore volume, uniform microporous channels, and excellent thermal and hydrothermal stability (Koohsaryan and Anbia, 2016). Some of them are super-hydrophilic and have well-defined sub-nanometer pores, which provide preferential flow paths for water (Fathizadeh et al., 2011). Benefitting from that, the addition of zeolite nanoparticles would enhance the membrane water permeability without reducing salt rejection substantially.

β zeolite is well known with its three-dimensional 12-membered ring (12R) microporous structure and well acidic sites as solid acid catalyst (Huang et al., 2017). The microporous structure endows them bigger sub-nanopores (7.5 Å) than other zeolite nanoparticles (Taborda et al., 2011). The inner-nano-porous of β zeolite in the PA matrix could supply extra channels to the water (Paul and Jons, 2016). Moreover, β zeolite nanoparticles with highly electronegative (Suárez et al., 2019) could enhance the zeta potential of membrane surface, and result in the improvement of membrane separation performance. It also can maintain stability in structure and properties during post-treatment because of their excellent thermal stability.

Therefore, in this work, a hydrophilic β zeolite nanoparticle was utilized as the additive into the aqueous phase to fabricate a high flux NF membrane via IP. A series of TFN membranes with different β zeolite loadings were fabricated for the investigation of the effect of β zeolite concentration in the aqueous phase. Following the preparation, attention has been paid to the membrane characterizations. The NF membrane characteristics involving surface structural morphology, surface charge and surface hydrophilicity of such membrane at different β zeolite nanoparticle loading was conducted. Separation tests were also implemented to evaluate the water permeability and the separation performance of mono and divalent salts.

1. Materials and methods

1.1. Materials

The substrate-polyether sulfone (PES, MW=30,000 Da) UF membranes were purchased from Advanced Membrane Technology INC (Beijing) Co. Ltd. (China). β zeolite nanoparticles were supplied by Nanjing XFNANO technology Co. Ltd. (China). Piperazine (PIP) and 1,3,5-benzenetricarbonyl trichloride (TMC, >98%) were purchased from Aladdin Industrial Co., Ltd. (Shanghai, China). n-hexane was obtained from Beijing chemical works (China). Sodium sulfate (Na_2SO_4) (>99%, AR), sodium chloride (NaCl) (>99.8%, GR), magnesium sulfate ($MgSO_4$) (>98%, AR) and magnesium chloride ($MgCl_2$) (>99%, AR) were purchased from Sinopharm Chemical Reagent Co., Ltd. (Shanghai, China). DI water(0.1–1 μS/cm) was obtained from the laboratory.

1.2. Fabrication of NF composite membranes modified with β zeolite

The NF composite membranes were fabricated by forming a PA selective layer via IP on the surface of an asymmetric PES UF membrane. The main preparation procedures were as follows:

The recipes of several TFC and TFN membranes in this study are detailed in Table 1. Firstly, a certain amount of β zeolite, 1% TEA and 16% phosphoric acid were added into 1% PIP solution. Then the solution was sonicated with an ultrasonic cell disrupter (SCIENTZ, JY92-IIN) about 1 hr as the aqueous solution. Meanwhile, 0.2% TMC was dissolved in n-hexane via ultrasonic dissolving method for 1 hr as the organic solution. Then 30 mL aqueous solution was poured slowly on the PES porous substrate for 3 min to allow the amine solution penetrate into the pores of the substrate. Subsequently, the excess solution on the PES supports were removed by a rubber roller. Then the monomer-saturated support membrane was soaked in organic solution for 30 sec, resulting in the formation of a TFC PA layer, and then the pristine membranes were dried in the air. Next, the as-fabricated TFC/TFN membranes were cured in an oven (ASCARI, 101–2A) at 80 °C for 3 min respectively. Finally, the membrane samples were rinsed and stored in DI at 4 °C until use.

1.3. Characterization methods

1.3.1. Characterization of β zeolite

The morphology properties of β zeolite was measured by Transmission electron micrograph (TEM, H-7500, Japan) and Field emission scanning electron microscopy (FE-SEM, SU8020, Japan). The crystal form of β zeolite was measured with an X-ray diffractometer (XRD, Rigaku smartlab (9), Japan).

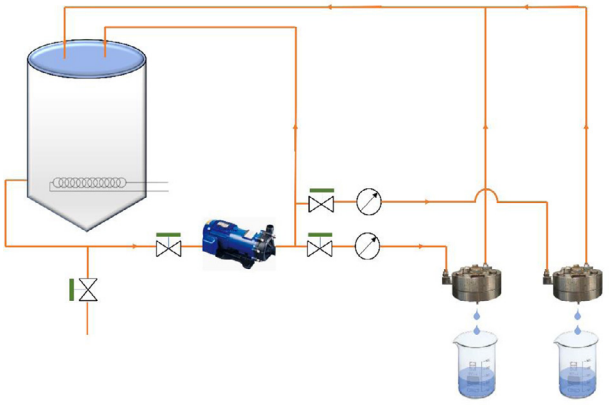

Fig. 1 – The schematic of cross-flow setup for NF membrane separation performance tests. (1) feed tank, (2) temperature control unit, (3) membrane cells (*d*=5.78 cm), (4) (5) pressure gauges, (6) vacuum pump, (7) regulating valves, (8) discharge gate.

An electrophoretic mobility measurement (Zetasizer Nano-ZS, Malvern, England) was used to obtain the surface zeta potentials of β zeolite nanoparticles.

1.3.2. *Characterization of TFC and TFN membranes*

Field emission scanning electron microscopy (FE-SEM, SU8020, Japan) was used to analyze the membrane morphological structure. The surface chemical structure of the PA layers was characterized by energy-dispersive X-ray (EDX) and X-ray photoelectron spectroscopy (XPS, ESCALAB 250Xi, Thermo Fisher, USA) to determine the distribution state of β zeolite in the whole membrane. The surface roughness of the prepared membranes was examined by an atomic force microcopy (AFM, SPM-970). The scanned area of the prepared membranes was 5 μm × 5 μm. The mean roughness (Ra) was reported to state the difference of the membrane surface topology. The water contact angle, characterized the hydrophilicity of the membrane surface, was measured by a contact angle meter (OCA20, Germany). The equilibrium value was the average of left and right angles. The reported contact angle values were the average of three measurements of each membrane sample. The surface charge properties of the TFN and TFC membranes were measured by a zeta potential analysis meter (Anton Paar, Austria). Every membrane was measured in 0.001 mol/L potassium chloride solution at 25 °C. The electric conductivity of test solution was measured by a conductivity meter (S230).

1.4. *Separation performance tests of membranes*

The NF membrane performance including the permeability and rejection were evaluated using a cross-flow setup (Fig. 1) at room temperature. The effective membrane area in the membrane cell was about 26.23 cm^2. 2 g/L of Na_2SO_4, $MgSO_4$, $MgCl_2$ and NaCl salt solution were used as feed solutions, respectively. All the membranes were preconditioned at 1.0 MPa for 0.5 hr until getting a stable water flux. Then the volume of filtrate was measured at 0.2 MPa. Three trials were carried out for each membrane test to guarantee the accuracy of the results. The final results presented are an average of the three measured values. The water flux F (L $m^{-2}hr^{-1}$) was determined by dividing the permeate volume V (L) by the effective membrane area A (m^2), filtration time t (hr) according to Eq. (1)

$$F = \frac{V}{At} \tag{1}$$

The salt rejection R (%) was calculated by Eq. (2), where C_p and C_f were the salt concentrations in the permeate and feed solutions, respectively. Salt concentration can be converted into the electric conductivity in proportion within a certain range (Zhang et al., 2019). Therefore, in this work, the salt concentration was replaced with the electric conductivity.

$$R = \left(1 - \frac{C_p}{C_f}\right) \times 100\% \tag{2}$$

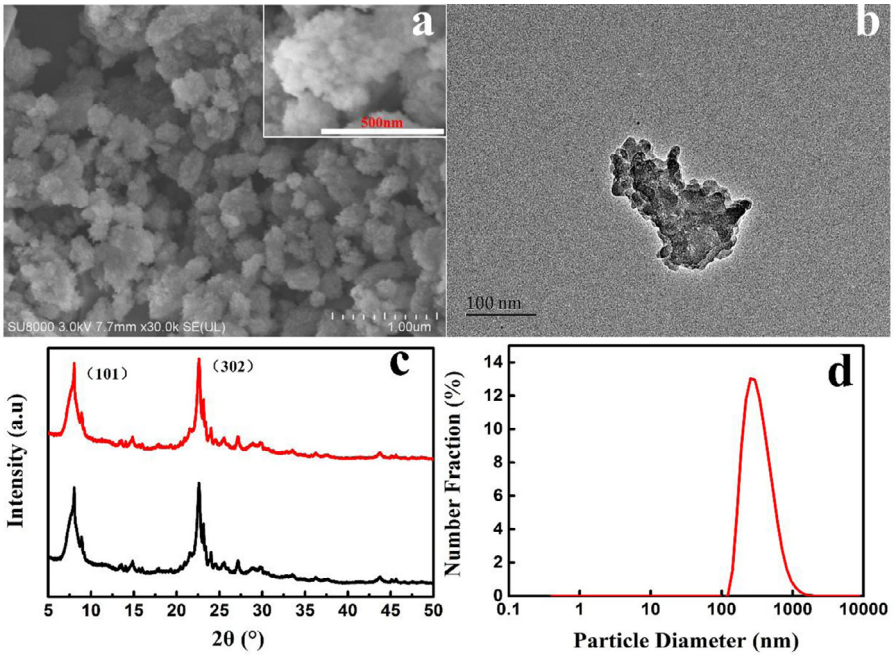

Fig. 2 – Characterizations of β zeolite nanoparticles: (a) FE-SEM image, (b) TEM image, (c) XRD pattern, and (d) particle size.

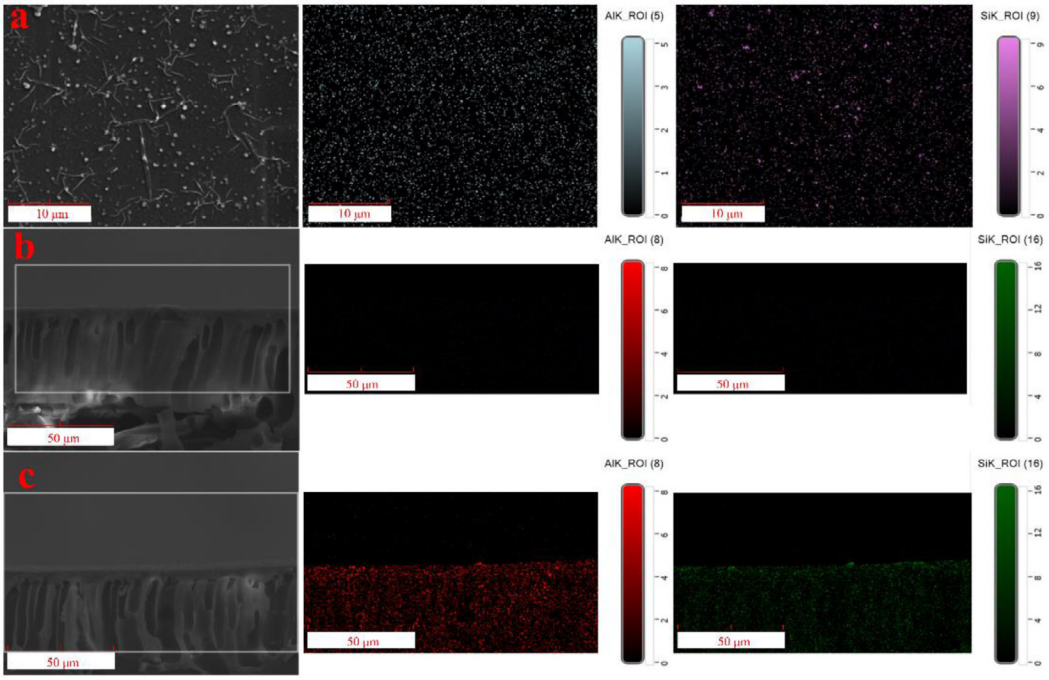

Fig. 3 – SEM-EDX images of membranes (a) TFN2.0wt% membrane surface, (b) TFC membrane cross-sectional scan image and (c) TFN2.0wt% membrane cross-sectional scan image.

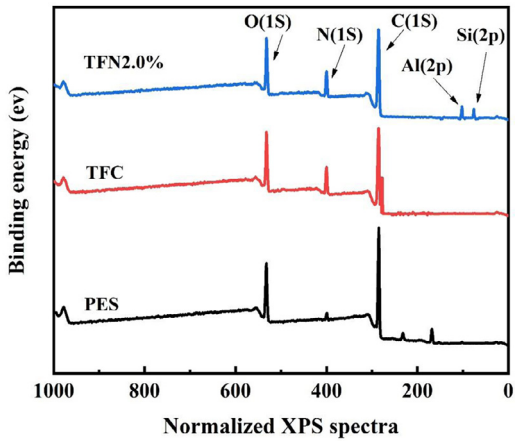

Fig. 4 – XPS survey spectra for the three type of membranes.

2. Results and discussion

2.1. *Characterization of β zeolite*

The morphologies, crystal form and size distribution of β zeolite nanoparticles are shown in Fig. 2. It can be seen in the SEM images (Fig. 2a) that the β nanoparticle crystals had irregular shapes and most of them showed particle sizes ranging from 100 nm to 1000 nm. The particle diameter of β zeolite was shown in (Fig. 2d) and the average diameter was measured to be 465.4 nm. TEM graphic further illustrated the structural properties of β samples, which presented the irregular nanoparticle crystals. A small crystal (˜200 nm) was observed for β zeolite nanoparticle (Fig. 2b), which was consistent with the FE-SEM images (Fig. 2a). A few spot lights were observed on the irregular shaped nanocrystals, which was indicative of small amount of micropores. Fig. 2c displays the XRD patterns of β zeolite samples before and after ultrasonic treatment. Two most significant diffraction peak at $2\theta = 7.8°$ (101), 22.4° (302) of the typical BEA structure were exhibited, which manifests the crystallinity could be well kept after the ultrasonic treatment (Gao et al., 2019).

2.2. *Surface morphology of the membranes*

The β zeolite were well dispersed on the external membrane surface and no obvious agglomeration of nanoparticles were observed as shown in Fig. 3a. Moreover, Si and Al elements were distinctly observed on the TFN2.0wt% membrane cross-sectional scan image, while barely on the TFC membrane (Fig. 3b-c). It indicated that β zeolite nanoparticles were introduced into the TFC membrane surface successfully. It has been reported that most of zeolite nanoparticles were encapsulated in the PA layer. The same results were characterized in this research as shown in Fig. 4. It manifested that few β zeolite nanoparticles could stick out of the PA selective layer. From the wide scan spectra of the three type of membranes, the emission peaks at 285.44, 400.08 and 531.79 eV were ascribed to be the binding energies of C 1 s, N 1 s and O 1 s, respectively. The contents of the aluminum Al and silicon Si elements were 0.27% and 1.82% respectively for TFN2.0wt% membrane which shown as a lower emission peaks at 74 eV and 99 eV on the scan spectra.

Fig. 5 shows the SEM images of synthesized TFC and TFN membranes. As shown in the SEM image (Fig. 5a), the pristine membrane surface exhibited a typical homogeneous wrinkle structure, which indicated the TFN membrane was successfully fabricated (Tan et al., 2018). Besides, it's obvious that the Turing-type structure on the membrane surface was changed with the addition of β zeolite. It suggested that, to some extent, the diffusion of the aqueous phase to the reaction zone was affected by the introduction of β zeolite nanoparticles (Li et al., 2017). When the β zeolite loading increased from 0.5 wt% to 2.0 wt%, the wrinkles on the TFN membrane surface be-

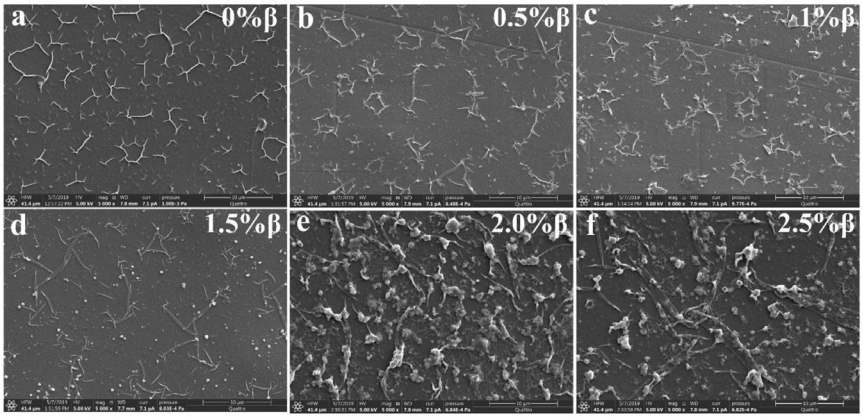

Fig. 5 – SEM images of surface view of TFC and TFN membranes with different zeolite loadings. (a) TFC membrane, (b) TFN0.5% membrane, (c) TFN1% membrane, (d) TFN1.5%membrane, (e) TFN2% membrane and (f) TFN2.5% membrane.

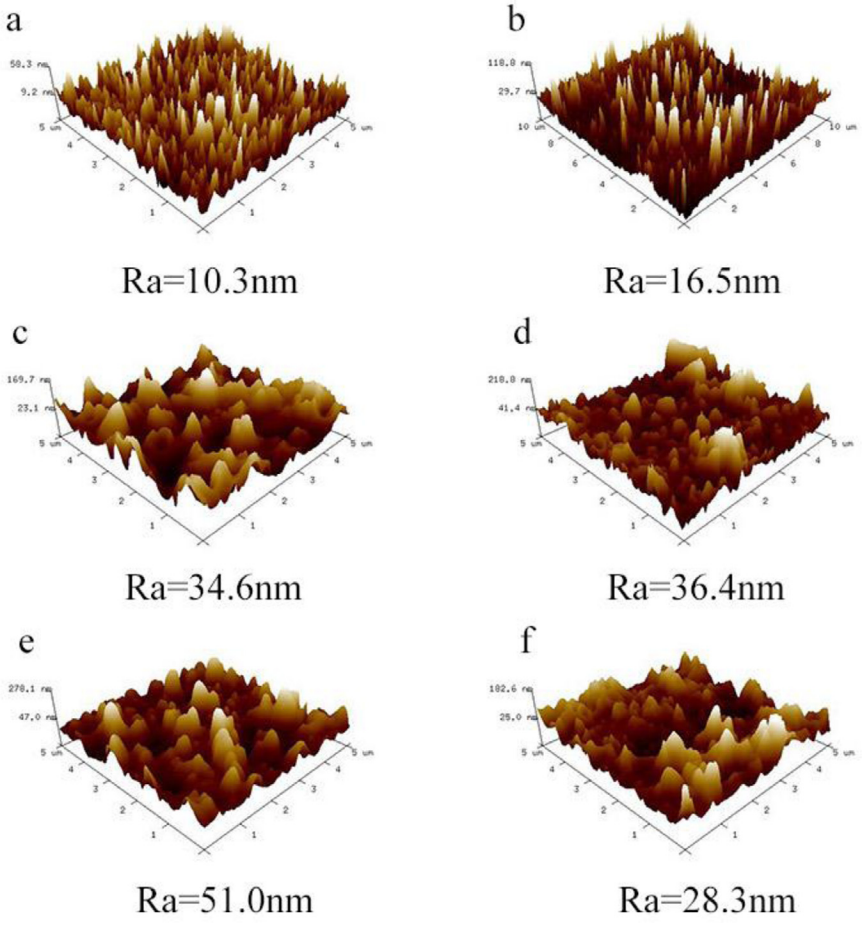

Fig. 6 – AFM characterization of (a) TFC membrane, (b) TFN0.5% membrane, (c) TFN1% membrane, (d) TFN1.5% membrane, (e) TFN2% membrane and (f) TFN2.5% membrane.

came larger and coarser. Bigger Turing-type structure would increase the surface area and hence higher water flux. Therefore, the measured average root mean square roughness (Ra) which represents the surface area were shown in Fig. 6, which was consistent with the changes of structure. In addition, the wrinkles were still distributed evenly on the membrane surface. However, when the content of β zeolite nanoparticle loading grew to 2.5%, the nanoparticles were dispersed unevenly and agglomerated. The agglomeration of nanoparticles would be a physical obstruction for diffusion of diamine solution to organic phase (Wen et al., 2017). Consequently, it would reduce the reaction rate of PIP and increase the generation of defects on the membrane surface. Moreover, overcrowded nanoparticles would also reduce the effective sub-nanopores of β zeolite, thereby decrease the water flux of the membranes. These changes on surface structure clearly show that the

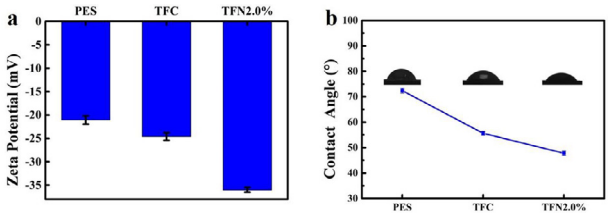

Fig. 7 – The results of the surface zeta potential (a) and the contact angle (b) of membrane samples.

addition of β zeolite will affect the IP procedure of PIP and TMC, resulting in the surface morphology changes.

To further investigate the surface morphology of the membrane, AFM analysis was used to characterize the membrane surface roughness. Previous studies reported that membrane surface roughness had significant influence on the water permeation flux (Abdikheibari et al., 2018; Lai et al., 2018). Therefore, the effect of β zeolite nanoparticles on membrane surface roughness was studied and shown in Fig. 6. Introduction of β zeolite nanoparticles into the PA selective layer considerably increased the membrane surface roughness. The Ra of pristine TFC membrane was 10.3 nm, which was a characteristic value of a TFC NF membrane with a relatively smooth surface. With the increase of β zeolite nanoparticle concentration from 0.5% to 2.0%, the Ra of TFN membranes increased gradually, which was mainly caused by the bigger and coarser wrinkles on the TFN membrane surface. However, when the content of β zeolite grew up to 2.5%, the Ra of the membrane dropped to 28.3 nm. It was because that the large clumps and the unevenly distribution of the nanoparticles resulting in surface roughness reduction, which was consistent with the SEM results (Fig. 5f). Increased surface roughness had a positive effect on the water permeability by increasing the effective surface area available for water molecules to permeate (Liu and Chen, 2013).

2.3. *Zeta potential and hydrophilicity of the membranes*

As we known, Donnan exclusion and size exclusion effect are the main separation mechanisms of the membrane (Anand et al., 2018; Donnan, 1995). Thus, membrane surface charge had great influence on membrane separation properties. In this work, the surface charge properties of the membranes were evaluated by surface zeta potentials. According to the results in Fig. 7a, all the membrane surfaces were negatively charged. The magnitude of the negative zeta potentials follows the order of TFN2.0% > TFC > PES membranes. The original TFC membrane surface was more negatively charged than the PES substrate. It was because the PA selective layer of TFN membrane inherently possesses an outer layer of fixed negative charges, which were endowed by the carboxyl groups hydrolyzed from unreacted acyl chlorides of TMC (Boo et al., 2018). The negative charge of TFN2.0% membrane surface was more intensified. It was attributed to the introduction of β zeolites whose surface were high negatively charged (-37.8±1.2 mV.). It was reported that the negative charge of the NF membrane surface could cause a stronger electrostatic exclusion effect on SO_4^{2-} than Cl^-, because of the Donnan exclusion effect (Pan et al., 2017). Thereby, the separation effect of SO_4^{2-} and Cl^- would be enhanced, when the membrane surface became more negatively charged.

Fig. 7b indicates the water contact angle of the three kinds of membranes, which represents the hydrophilicity of the membrane surface. The smaller the contact angle, the stronger the wetting ability and the better the hydrophilicity. Compared with the pristine TFC membrane (55.6°), the water contact angle of the TFN2.0% membranes were lower (47.8°), which was owing to the hydroxyl group on the β zeolite surface. It indicated that the membrane surface became more hydrophilic because of the introduction of the β zeolite nanoparticles. Besides, According to the analysis results of Cassie-Baxter model, the increase of the roughness will enhance the hydrophilicity of membrane surface when the membrane surface is hydrophilic. In contrary, when the membrane surface is hydrophobic, the increase of the roughness renders the membrane surface more hydrophobic. Therfore, the improved hydrophilicity was also attributed to the increased surface roughness (Liu et al., 2019). A more negatively charged and hydrophilic surface endowed the membrane a better separation performance. Thus, the addition of β zeolite would attribute to fabricating a high-flux and high-separation performance membrane.

2.4. *Separation performance of the membrane*

The separation performances of NF composite membranes were evaluated at 0.2 MPa. The result (Fig. 8a) illustrates the effect of different β zeolite loadings on membrane pure water flux. It is clear that pure water flux increased with the β zeolite loading growing until 2.0 wt%. In particular, the TFN membrane exhibited the highest water permeability of 81.22 L m^{-2} hr^{-1} when 2.0% β zeolite was introduced, which enhanced more than twice as much as the flux of TFC membrane (34.06 L m^{-2} hr^{-1}). The addition of β zeolite was conducive to improve the water flux. It could be due to the inner nanopores of the β zeolite, which was supposed to provide more permeation channels to water compared with the PA layer. The size of β zeolite nanopores used in this experiment was 0.5-0.7 nm, which was larger than the 0.27 nm of water molecules and hence can transit it apparently (Song et al., 2020). Furthermore, the β zeolite nanoparticles influence the IP procedure to enhance the PA layer permeation performance due to the change of membrane surface morphology (Ma et al., 2012). There are more and more wrinkles on the membrane surface, when increasing the β zeolite loadings. In addition, the wrinkles on the TFN membranes grew bigger and coarser as mentioned before in SEM and AFM (Figs. 5 and 6). It could increase the effective surface area available for water molecules to permeate thus the enhancement of the membrane water flux. Moreover, increased surface hydrophilicity was also the important reason for the water permeation improvement. However, when the content of the β zeolite increased to 2.5%, the membrane flux was declined to 70.74 L m^{-2} hr^{-1}. It meant the further increase of β zeolite content had a passive influence on the permeability of TFN membranes. On the one side, it was because the PA layer became much thicker. The thicker the selective layer, the lower the membrane water permeant ability. On the other side, the high content of β nanoparticle was liable to cause the serious aggregation (as showed in the SEM analysis), which would reduce the effective sub-nanopores of β zeolite that allow water molecules to pass through. Thus, the excess loading of β zeolite nanoparticles would lead to the decline of the TFN membranes flux.

Figs. 8b-9 present the separation performance in four different salt solutions of the membranes. The membrane solute permeability (Fig. 8b) presented similar variation tendency with pure water flux as showed in Fig. 8a. The differences of salt rejection between four different solutions were shown in Fig. 9, which investigated the effect of β zeolite loadings. The results changed in the following order: Na_2SO_4 > $MgSO_4$ > $MgCl_2$ > NaCl, which conformed to the characteristic of typical negatively charged nanofiltration membrane (Ren et al., 2019). All membranes were negatively charged based on the results of zeta potential measurements. Generally, For most electrolytes, the separation performance of NF membranes is determined by electric density, ion size (hydration radius),

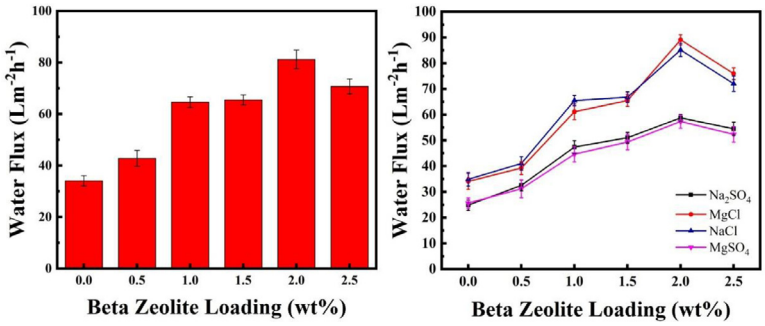

Fig. 8 – Effect of β zeolite loading on (a) pure water flux, (b) salt water flux.

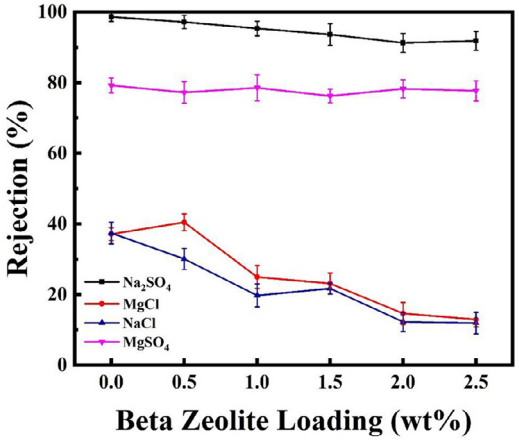

Fig. 9 – Effect of β zeolite loading on salt rejection.

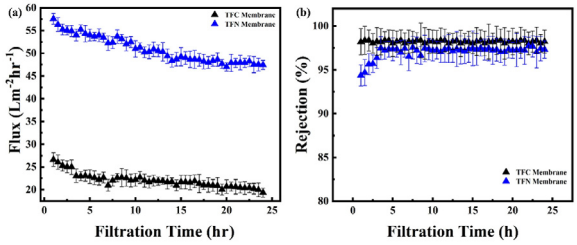

Fig. 10 – (a) The changes of membrane water permeat flux under long-term operation (b) the changes of membrane rejection under long-term operation.

and ion diffusion coefficient (Gu et al., 2008).For cations, although the hydration radius of Mg^{2+}(0.428 nm) is larger than that of Na^{+}(0.358 nm), the attraction between the positively charged cations and the negatively charged membrane surface is stronger, making Na_2SO_4 have a higher repulsion than $MgSO_4$. Membrane pore size has become larger and the structure become looser with the increase of β zeolite(Jeong et al., 2007). The rejection to Na_2SO_4 decreased slightly with increasing the loading of β zeolite because of the smaller hydration radius, higher diffusion coefficient ($1.33*10^{-9}$ m^2sec^{-1}) of Na^{+} (An et al., 2011). However, the loading of β zeolite has no great effect on the rejection to $MgSO_4$ due to the larger hydration radius and lower diffusion coefficient($0.70*10^{-9}$ m^2sec^{-1}) of Mg^{2+}. As for NaCl and $MgCl_2$, Both the two rejection decreased when the concentration of β zeolite increased. This was ascribed to the higher diffusion coefficient and smaller hydration radius of Na^{+}, meanwhile the smaller hydration radius (0.12 nm) and the lower surface charge of Cl^{-} for NaCl. At the same time, stronger attraction between Mg^{2+} and the membrane surface, and the lower repulsion of Cl^{-} and the membrane surface are the reason for the reduction of $MgCl_2$. Therfore, the data also indicated the efficiency of salt separation of monovalent and divalent salt increased with the increase of β zeolite loadings. It's the result of enhanced Donnan exclusion effect between membrane surface and solutes as mentioned in the surface zeta potential (Fig. 7a).

As shown in Fig. 8a-b, the stability of membrane separation performance was investigated by 2 g/L of Na_2SO_4 at 0.2 MPa. For both the two kinds of membranes, the water permeate flux decreased after continuous operation for 24 hr (Fig. 8a). When investigated by the Na_2SO_4 solutions, the membrane permeate flux was prone to decrease sharply due to the unstable performance of membranes in the early stage (3–3.5 hr). The water flux of TFC membrane decreased from 26.64 to 22.95 L m^{-2} hr^{-1}, while the TFN membrane decreased from 57.62 to 54.03 L m^{-2} hr^{-1}. Subsequently, during the stablility test for 24 hr, the water permeate flux of TFC membrane decreased slowly from 22.95 to 19.36 L m^{-2} hr^{-1}, while the other one decreased from 54.03 to 47.44 L m^{-2} hr^{-1}. it is because the pore system and surface double-electron layer got thinner which resulted in the shrinkage of the three-dimensional network structure of the membrane after the deposition of salt ions on the membrane surface during the long-term operation. In addition, for both the two kinds of membranes, the rejection of Na_2SO_4 was relatively stable, which maintained 98.35% and 97.59% respectively (Fig. 1R5b). However, at the beginning of operation, the rejection of TFN membrane increased significantly, from 94.36% to 97.59%. This is because the loose structure of TFN membrane has been compacted to be denser during the operation and lead to the increasement of rejection. The result demonstrates that TFN membrane was stable within the experimental range. At the same time, it also indicates that the β zeolite nanoparticles could exist stably on the surface of the membranes, and wouldn't be lost or cause the damage to the membrane structure easily. All this was attributed to the excellent mechanical and hydrothermal stability of β zeolite nanoparticles. It also shows that most of the β zeolite was encased stably in the PA selective layer rather than exposed to the membrane surface.

Thin-film nanocomposite (TFN) nanofiltration (NF) membraneswere prepared using hydrophilic SiO_2 (HGPN-SiO_2) nanoparticles as the inorganic modifying monomer by an interfacial polymerization (IP) process. the permeate flux of the TFN-NF membrane was twice that of the pure NF membrane at 0.4 MPa. But at the same time, the rejection to inorganic salt all decreased (Wei et al., 2019). Rajaeian et al. (2013) prepared the TFN membrane using an modified TiO_2. The experimental results showed that the pure water flux increased progressively from 11.2 L m^{-2} hr^{-1} of TFC membrane to 27 L m^{-2} hr^{-1}

of TFN membranes when tested at 7.5 bar. For the TFN membrane prepared in our research, the water permeate flux could be increased by twice as much as that of TFC membrane at 0.2 MPa. At the same time, the separation efficiency of monovalent and divalent ions was improved. These results were attributed to the sub-nanopores of the Beta zeolite which could supply extra selective channels for water molecules. Therefore, membrane water flux of the TFC membrane could increase at low operation pressure.

3. Conclusion

A negatively charged thin film composite NF membrane modified with β zeolite was prepared by interfacial polymerization. It exhibited a higher water flux and better salt separation characteristics compared to the TFC membrane. Moreover, the surface roughness, hydrophilicity and electronegativity of the modified TFC membrane were improved with the increase of β zeolite loadings at relatively lower concentration. The pure water flux of the modified TFC membrane reached to 81.22 L m^{-2} hr^{-1} at 0.2 MPa which was improved more than twice as much as the flux of TFC membrane. The salt separation performance of monovalent and divalent salt was enhanced at the same time. Our research further proved the positive effect of β zeolite on preparing of high flux membranes and expanded the application field of β zeolite. This study supplied a novel route to fabricate the modified TFC membrane with high flux and outstanding salt separation, which is possible to be used to treat the organic and inorganic mixed wastewater.

Acknowledgments

This work was supported by the National Natural Science Foundation of China (Nos. 21476248, 21878323), and the Youth Innovation Promotion Association of CAS (No. 2011039).

REFERENCES

Abdikheibari, S., Lei, W., Dumée, L.F., Milne, N., Baskaran, K., 2018. Thin film nanocomposite nanofiltration membranes from amine functionalized-boron nitride/polypiperazine amide with enhanced flux and fouling resistance. J. Mater. Chem. 6, 12066–12081.

Ahmad, A.L., Abdulkarim, A.A., Ooi, B.S., Ismail, S., 2013. Recent development in additives modifications of polyethersulfone membrane for flux enhancement. Chem. Eng. J. 223, 246–267.

An, Q., Li, F., Ji, Y., Chen, H., 2011. Influence of polyvinyl alcohol on the surface morphology, separation and anti-fouling performance of the composite polyamide nanofiltration membranes. J. Memb. Sci. 367, 158–165.

Anand, A., Unnikrishnan, B., Mao, J.Y., Lin, H.J., Huang, C.C., 2018. Graphene-based nanofiltration membranes for improving salt rejection, water flux and antifouling–a review. Desalination 429, 119–133.

Andrade, P.F., de Faria, A.F., Oliveira, S.R., Arruda, M.A.Z., Gonçalves, M.D. C., 2015. Improved antibacterial activity of nanofiltration polysulfone membranes modified with silver nanoparticles. Water Res. 81, 333–342.

Boo, C., Wang, Y., Zucker, I., Choo, Y., Osuji, C.O., Elimelech, M., 2018. High performance nanofiltration membrane for effective removal of perfluoroalkyl substances at high water recovery. Environ. Sci. Technol. 52, 7279–7288.

Donnan, F.G., 1995. Theory of membrane equilibria and membrane potentials in the presence of non-dialysing electrolytes. A contribution to physical-chemical physiology. J. Memb. Sci. 100, 45–55.

Fathizadeh, M., Aroujalian, A., Raisi, A., 2011. Effect of added NaX nano-zeolite into polyamide as a top thin layer of membrane on water flux and salt rejection in a reverse osmosis process. J. Memb. Sci. 375, 88–95.

Gao, K., Wang, Q., Du, X., Wei, Q., Huang, Y., 2019. Microporous and mesoporous materials efficient adsorption and eco-environmental oxidization of dimethylamine in beta zeolite. Micro. Meso. Mater. 282, 219–227.

Gu, S., He, G., Wu, X., Guo, Y., Liu, H., Peng, L., et al., 2008. Preparation and characteristics of crosslinked sulfonated poly (phthalazinone ether sulfone ketone) with poly (vinyl alcohol) for proton exchange membrane. J. Memb. Sci. 312, 48–58. https://doi.org/10.1016/j.memsci.2007.12.053.

Heinz, H., Pramanik, C., Heinz, O., Ding, Y., Mishra, R.K., Marchon, D., et al., 2017. Surface science reports nanoparticle decoration with surfactants : molecular interactions, assembly, and applications. Surf. Sci. Rep. 72, 1–58.

Huang, G., Ji, P., Xu, H., Jiang, J.G., Chen, L., Wu, P., 2017. Fast synthesis of hierarchical Beta zeolites with uniform nanocrystals from layered silicate precursor. Micro. Meso. Mater. 248, 30–39.

Jeong, B., Hoek, E.M.V, Yan, Y., Subramani, A., Huang, X., Hurwitz, G., et al., 2007. Interfacial polymerization of thin film nanocomposites : a new concept for reverse osmosis membranes. J. Memb. Sci. 294, 1–7.

Kango, S., Kalia, S., Celli, A., Njuguna, J., Habibi, Y., Kumar, R., 2013. Progress in polymer science surface modification of inorganic nanoparticles for development of organic – inorganic nanocomposites — a review. Prog. Polym. Sci. 38, 1232–1261.

Koohsaryan, E., Anbia, M., 2016. Nanosized and hierarchical zeolites: a short review. Cuihua Xuebao/Chinese J. Catal. 37, 447–467.

Lai, G.S., Lau, W.J., Goh, P.S., Ismail, A.F., Tan, Y.H., Chong, C.Y., et al., 2018. Tailor-made thin film nanocomposite membrane incorporated with graphene oxide using novel interfacial polymerization technique for enhanced water separation. Chem. Eng. J. 344, 524–534.

Lalia, B.S., Kochkodan, V., Hashaikeh, R., Hilal, N., 2013. A review on membrane fabrication: structure, properties and performance relationship. Desalination 326, 77–95.

Lau, W.J., Ismail, A.F., Goh, P.S., Hilal, N., Ooi, B.S., 2015. Characterization methods of thin film composite nanofiltration membranes. Sep. Purif. Rev. 44 (2), 135–156.

Liu, J., Wang, Q., Shan, H., Guo, H., Li, B., 2019. Surface hydrophobicity based heat and mass transfer mechanism in membrane distillation. J. Memb. Sci. 580, 275–288.

Li, X., Zhao, C., Yang, M., Yang, B., Hou, D., Wang, T., 2017. Applied surface science reduced graphene oxide-NH_2 modified low pressure nanofiltration composite hollow fiber membranes with improved water flux and antifouling capabilities. Appl. Surf. Sci. 419, 418–428.

Liu, Y., Chen, X., 2013. High permeability and salt rejection reverse osmosis by a zeolite nano-membrane. Phys. Chem. Chem. Phys. 15, 6817–6824.

Lv, Y., Yang, H.C., Liang, H.Q., Wan, L.S., Xu, Z.K., 2016. Novel nanofiltration membrane with ultrathin zirconia film as selective layer. J. Memb. Sci. 500, 265–271.

Lyu, S., Chen, W., Zhang, W., Fan, Y., Jiao, W., 2015. Wastewater reclamation and reuse in China : opportunities and challenges. J. Environ. Sci. 39, 86–96.

Ma, N., Wei, J., Liao, R., Tang, C.Y., 2012. Zeolite-polyamide thin film nanocomposite membranes: Towards enhanced performance for forward osmosis. J. Memb. Sci. 405–406, 149–157.

Mohammad, A.W., Teow, Y.H., Ang, W.L., Chung, Y.T., Oatley-Radcliffe, D.L., Hilal, N., 2015. Nanofiltration membranes review: Recent advances and future prospects. Desalination 356, 226–254.

Oatley-radcli, D.L., Walters, M., Ainscough, T.J., Williams, P.M., Wahab, A., Hilal, N., 2017. Nano filtration membranes and processes: a review of research trends over the past decade. J. Water Process Eng. 19, 164–171.

Pan, Y., Xu, R., Lü, Z., Yu, S., Liu, M., Gao, C., 2017. Enhanced both perm-selectivity and fouling resistance of poly(piperazine-amide) nanofiltration membrane by incorporating sericin as a co-reactant of aqueous phase. J. Membr. Sci. 523, 282–290.

Paul, M., Jons, S.D., 2016. Chemistry and fabrication of polymeric nanofiltration membranes: a review. Polymer 103, 417–456.

Rajaeian, B., Rahimpour, A., Tade, M.O., Liu, S., 2013. Fabrication and characterization of polyamide thin film nanocomposite (TFN) nanofiltration membrane impregnated with TiO_2 nanoparticles. Desalination 313, 176–188.

Ren, Y., Zhu, J., Cong, S., Wang, J., Bruggen, B.V.D., Liu, J., et al., 2019. High flux thin film nanocomposite membranes based on porous organic polymers for nanofiltration. J. Memb. Sci. 585, 19–28.

Song, X., Wang, Y., Jiao, C., Huang, M., Wang, G., Jiang, H., 2020. Microstructure regulation of polyamide nanocomposite membrane by functional mesoporous polymer for high-efficiency desalination. J. Memb. Sci. 597, 117783.

Suárez, N., Pérez-pariente, J., Márquez-álvarez, C., Grande, M., 2019. Preparation of mesoporous beta zeolite by fluoride treatment in liquid phase. Textural, acid and catalytic properties. Micro. Meso. Mater. 284, 296–303.

Sumisha, A., Arthanareeswaran, G., Ismail, A.F., Kumar, D.P., Shankar, M.V., 2015. Functionalized titanate nanotube-polyetherimide nanocomposite membrane for improved salt rejection under low pressure nanofiltration. RSC Adv. 5, 39464–39473.

Taborda, F., Willhammar, T., Wang, Z., Montes, C., Zou, X., 2011. Synthesis and characterization of pure silica zeolite beta obtained by an aging – drying method. Micro. Meso. Mater. 143, 196–205.

Tan, Z., Chen, S., Peng, X., Zhang, L., Gao, C., 2018. Polyamide membranes with nanoscale turing structures for water purification. Science 80- (521), 518–521.

Wei, X., Xu, X., Wu, J., Li, C., Chen, J., Lv, B., et al., 2019. SiO_2 -modified nanocomposite nanofiltration membranes with high flux and acid resistance. J. Appl. Polym. Sci. 136, 1–11.

Wen, P., Chen, Y., Hu, X., Cheng, B., Liu, D., Zhang, Y., et al., 2017. Polyamide thin film composite nanofiltration membrane modified with acyl chlorided graphene oxide. J. Memb. Sci. 535, 208–220.

Zhang, Y., Zhao, C., Zhang, S., Yu, L., Li, J., Hou, L.A., 2019. Preparation of SGO-modified nanofiltration membrane and its application in SO_4^{2-} and Cl^- separation in salt treatment. J. Environ. Sci. 78, 183–192.

Zhou, D., Zhu, L., Fu, Y., Zhu, M., Xue, L., 2015. Development of lower cost seawater desalination processes using nano fi ltration technologies — a review. DES 376, 109–116.